

Punishment history biases corticothalamic responses to motivationally-significant stimuli

Federica Lucantonio, Zhixiao Su, Anna J. Chang, Bilal A. Bari, Jeremiah Y. Cohen

*The Solomon H. Snyder Department of Neuroscience, Brain Science Institute,
Kavli Neuroscience Discovery Institute, The Johns Hopkins University School of Medicine*

1 **Making predictions about future rewards or pun-
2 ishments is fundamental to adaptive behavior.
3 These processes are influenced by prior experi-
4 ence. For example, prior exposure to aversive
5 stimuli or stressors changes behavioral responses
6 to negative- and positive-value predictive cues.
7 Here, we demonstrate a role for medial pre-
8 frontal cortex (mPFC) neurons projecting to the
9 paraventricular nucleus of the thalamus (PVT;
10 mPFC→PVT) in this process. We found that a
11 history of punishments negatively biased behav-
12 ioral responses to motivationally-relevant stim-
13uli in mice and that this negative bias was asso-
14 ciated with hyperactivity in mPFC→PVT neu-
15 rons during exposure to those cues. Further-
16 more, artificially mimicking this hyperactive re-
17 sponse with selective optogenetic excitation of
18 the same pathway recapitulated the punishment-
19 induced negative behavioral bias. Together, our
20 results highlight how information flow within the
21 mPFC→PVT circuit is critical for making pre-
22 dictions about imminent motivationally-relevant
23 outcomes as a function of prior experience.**

24 Introduction

25 Effective decision making requires anticipating biologi-
26 cally significant outcomes associated with environmen-
27 tal stimuli. It also requires balancing the goals of a
28 decision—for instance, acquiring a reward or avoiding
29 a punishment—with certainty about the outcome of the
30 decision. For example, when the outcome of a decision to
31 approach or avoid a stimulus is ambiguous, the nervous
32 system must weigh the cost of receiving a punishment,
33 or missing out on a reward, with the benefit of obtaining
34 the reward, or avoiding the punishment.

35 Many decisions are influenced by background emo-
36 tional state. For example, both positive and negative

37 mood affect decision making (Deldin and Levin, 1986;
38 Wright and Bower, 1992; Bechara et al., 2000; Hockey
39 et al., 2000; Dolan, 2002; Harding et al., 2004). This
40 background state can be driven by prior experience. In
41 particular, prior exposure to aversive stimuli or stress-
42 tors changes behavioral responses to ambiguous stimuli
43 (Harding et al., 2004; Boleij et al., 2012; Rygula et al.,
44 2014). How the balance between competing behaviors is
45 weighed in the brain or how prior experience with an en-
46 vironment shifts this balance is still poorly understood.

47 The medial prefrontal cortex (mPFC) is critical for
48 regulating cue-mediated behaviors in both appetitive
49 and aversive domains (Ishikawa et al., 2008; Burgos-
50 Robles et al., 2009; Sotres-Bayon and Quirk, 2010;
51 Amemori and Graybiel, 2012; Burgos-Robles et al., 2013;
52 Courtin et al., 2014; Sangha et al., 2014; Sparta et al.,
53 2014; Burgos-Robles et al., 2017; Otis et al., 2017). Be-
54 havioral manifestations of appetitive and aversive condi-
55 tioning correlate with changes in neural activity within
56 the mPFC (Burgos-Robles et al., 2009; Peters et al.,
57 2009; Amemori and Graybiel, 2012; Burgos-Robles et al.,
58 2013; Moorman and Aston-Jones, 2015) and pharmacolog-
59 ical or optogenetic manipulations of mPFC alter both
60 reward-seeking and fear-related behaviors (Morgan and
61 LeDoux, 1995; Blum et al., 2006; Corcoran and Quirk,
62 2007; Sierra-Mercado et al., 2011; Sangha et al., 2014;
63 Sparta et al., 2014; Bari et al., 2019).

64 The mPFC has dense projections to subcortical struc-
65 tures involved in motivated behavior, including the
66 paraventricular thalamus (PVT; Vertes, 2004; Li and
67 Kirouac, 2012). Like the mPFC, PVT is recruited by
68 cues or contexts previously associated with rewarding or
69 aversive outcomes (Beck and Fibiger, 1995; Schiltz et al.,
70 2007; Yasoshima et al., 2007; Choi et al., 2010; Igelstrom
71 et al., 2010; Haight and Flagel, 2014; Hsu et al., 2014;
72 Do-Monte et al., 2015; Kirouac, 2015; Matzeu et al.,
73 2015; Penzo et al., 2015; Li et al., 2016; Zhu et al.,
74 2016; Do-Monte et al., 2017). PVT neurons are acti-

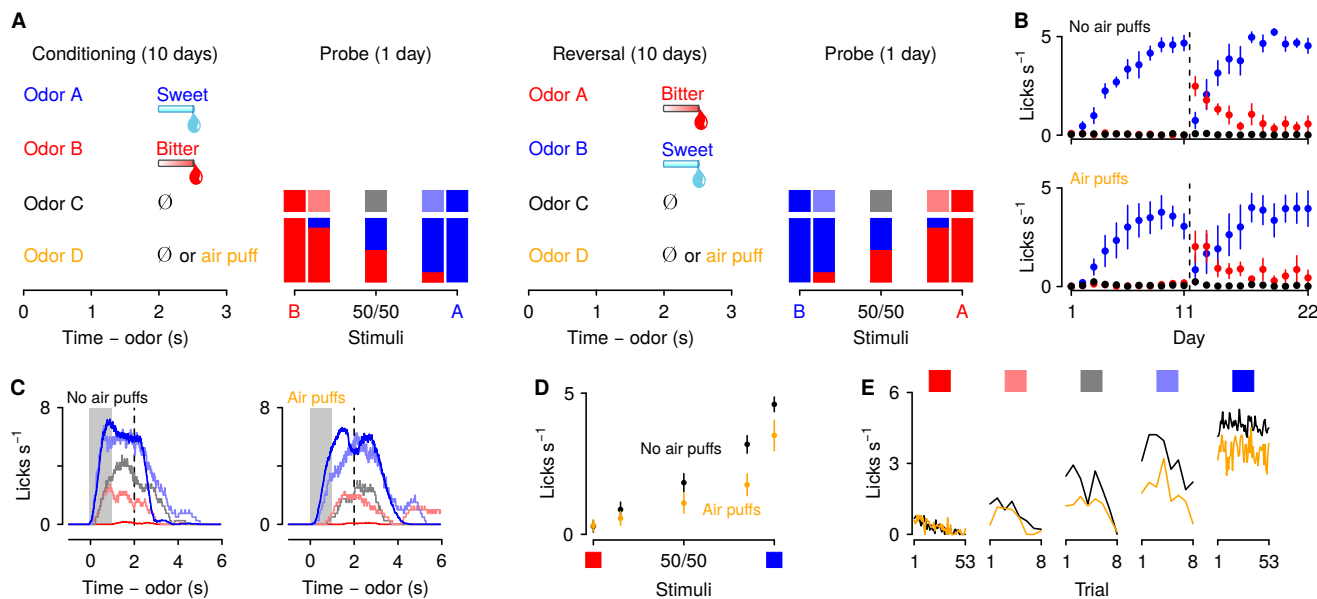


Fig. 1 | Behavioral responses to motivationally-significant predictive cues are modulated by punishment history. (A) Task design and experimental timeline. During ten conditioning sessions, odors (A, B, C and D) predicted an appetitive sucrose solution, an aversive denatonium solution, no outcome, and either no outcome or an unavoidable air puff, respectively. During the first probe test, A and B were mixed in three different ratios: 85% B/15% A (light red), 50% B/50% A (gray), 15% B/85% A (light blue). After completion of ten reversal training sessions, in which A and B contingencies were reversed, mice were re-trained in a second probe test. (B) Licking rates in no air puff (top, 7 mice) or air puff (bottom, 5 mice) groups across days, during odor and delay period, for sucrose (blue), denatonium (red), and no-outcome (black) trials. Dashed lines indicate reversals on day 11. (C) Licking behavior from a representative test session from a mouse without (left) and one with (right) exposure to air puffs. Color gradations between blue and red indicate odor mixtures as in (A). Gray bars indicate a period of odor presentation. Dashed lines indicate outcome delivery. (D) Licking rates during sucrose (blue square) and denatonium (red square) trials and during the eight probe trials for no air puff (black) and air puff (orange) groups, during odor and delay period. (E) Trial-by-trial licking rates during sucrose (blue square) and denatonium (red square) trials and during the eight probe trials for each ambiguous cue (light red, gray, light blue squares) for no air puff (black) and air puff (orange) groups, during odor and delay period. Line and error bars represent mean \pm SEM.

vated by multiple forms of stressors (Chastrette et al., 1991; Sharp et al., 1991; Cullinan et al., 1995; Bubser and Deutch, 1999; Spencer et al., 2004) and coordinate behavioral responses to stress (Hsu et al., 2014; Do-Monte et al., 2015; Penzo et al., 2015; Zhu et al., 2016; Do-Monte et al., 2017; Beas et al., 2018). On the other hand, under conditions of opposing emotional valence, PVT plays a role in multiple forms of stimulus-reward learning and PVT neurons have been reported to show reward-modulated responses (Schiltz et al., 2005; Igelstrom et al., 2010; Martin-Fardon and Boutrel, 2012; James and Dayas, 2013; Browning et al., 2014; Haight and Flagel, 2014; Li et al., 2016; Choi et al., 2019). Activity in mPFC neurons projecting to the PVT also suppresses both the acquisition and expression of conditioned reward seeking (Otis et al., 2017).

Taken together, these studies place the mPFC to PVT projection in a unique position to integrate information about positive and negative motivationally-relevant cues and translate it into adaptive behavioral responses. How these projection-specific prefrontal neurons regulate be-

havioral responses in ambiguous settings and how their neural activity may be altered upon presentation of a punishment is unknown.

To address these questions, we trained mice on a go/no-go discrimination task in which sweet- and bitter-predicting odor cues together with mixtures of varying proportions of those cues were concurrently presented to the mice and recorded extracellularly in single-cell mPFC and in identified mPFC \rightarrow PVT neurons. We then tested whether optogenetically stimulating mPFC \rightarrow PVT projections recapitulated the observed neuron-behavior relationships in those settings.

Results

Punishment history negatively biases behavioral responses to motivationally-significant stimuli. To assess the effect of punishment history on decisions about motivationally-significant outcomes, we developed a go/no-go discrimination task in head-fixed mice consisting of four phases: conditioning, probe test, reversal,

and a second probe test (Figure 1A). In the conditioning phase, four odor cues (A, B, C and D, counterbalanced) were presented. Odor A predicted an appetitive sweet solution ($3\text{ }\mu\text{l}$ of 5% sucrose water). Odor B predicted an aversive bitter solution ($3\text{ }\mu\text{l}$ of 10 mM denatonium water). Odor C was associated with no reinforcement. Odor D predicted a punishment (an unavoidable air puff delivered to the mouse's right eye) in mice assigned to the air puff group and was associated with no reinforcement in mice assigned to the no air puff group. Each behavioral trial began with an odor (1 s; conditioned stimulus, CS), followed by a 1-s delay and an outcome (unconditioned stimulus, US). Mice showed essentially binary responses to cues that predicted sucrose or denatonium. That is, they licked in anticipation of sucrose and did not in anticipation of denatonium. Thus, we designed a probe test, in which, in addition to the four conditioning odors, we measured behavioral responses to ambiguous stimuli. We designed parametrically-varying mixtures of stimuli between appetitive and aversive solutions. We exposed mice to unreinforced mixtures of varying proportions of odors A and B: 85%A/15%B, 50%A/50%B, 15%A/85%B. To ensure that behavioral responses to ambiguous stimuli were not driven by a mouse's preference for a particular odor, after completion of the probe test, cue-outcome associations for odors A and B were reversed, and each mouse was re-tested in a second set of probe stimuli.

As predicted, mice in both air puff and no air puff groups quickly learned the CS-US associations: they showed increases in anticipatory licking responses to the positive, sucrose-predicting cue and in the delay before sucrose arrived across conditioning sessions, while withholding licking after sampling the negative, denatonium-predicting cue (Figure 1B). Accordingly, a 3-factor ANOVA (session \times cue \times group) comparing licking behavior during sucrose and denatonium cue presentation and delay period demonstrated a significant main effect of session ($F_{1,9} = 29.74, p < 0.01$) and cue ($F_{1,1} = 64.77, p < 0.01$). Moreover, mice exposed to air puffs responded to the sucrose-predicting odor with fewer licks (cue \times group interaction, $F_{1,1} = 7.84, p < 0.05$). During reversal learning, in which A and B contingencies were reversed, mice in both no air puff and air puff groups quickly re-adapted to the new associations (Figure 1B). Accordingly, a 3-factor ANOVA (session \times cue \times group) comparing licking rates during sucrose and denatonium cue presentation and delay period demonstrated a significant interaction between cue and session ($F_{1,9} = 8.4, p < 0.01$).

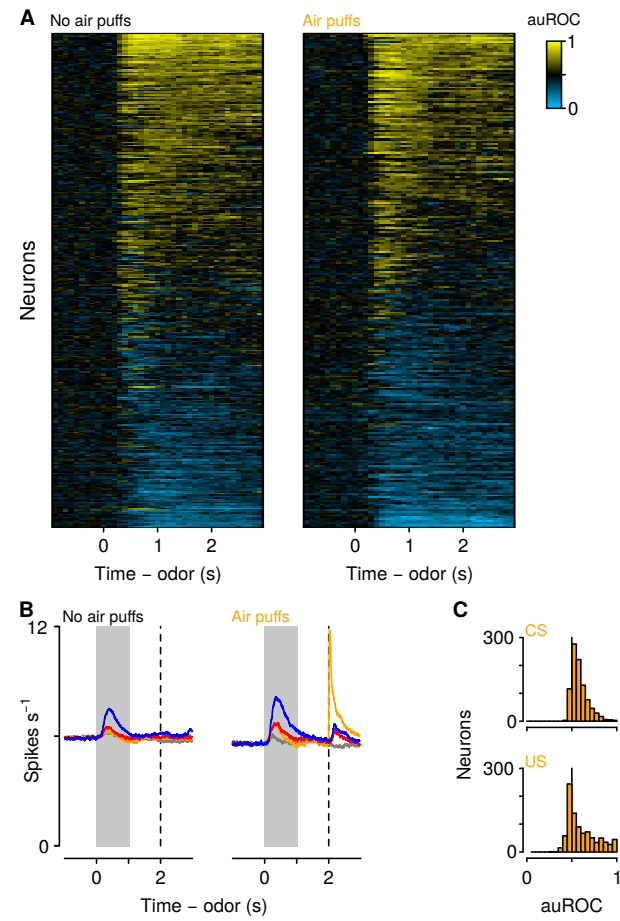


Fig. 2 | Neuronal responses across learning. (A) Discriminability (auROC) between sucrose and denatonium trials of all neurons in mice unexposed (left) and exposed (right) to air puffs. Increases (yellow) and decreases (cyan) in firing rate in sucrose trials relative to denatonium trials. Each row represents one neuron. (B) Average firing rates of all neurons with auROC values greater than 0.7 or less than 0.3 in at least one bin in no air puff (left) and air puff (right) mice during sucrose (blue), denatonium (red), no-outcome (gray) and air puff (orange) trials. Gray bars indicate a period of odor presentation. Dashed lines indicate outcome delivery. (C) auROC values for responses to air puff-predicting CSs (top) and air puff (bottom).

At the end of conditioning and reversal training, mice received a single probe test session. Behavioral responses from the initial probe test were not statistically different from data gathered in the second test and thus these sessions were analyzed together in the text. Licking rates for odor mixtures scaled with the proportion of the mixture that was the sucrose-predicting odor. This indicates that mice responded to parametrically varying ambiguous stimuli with smoothly varying behavioral responses (Figure 1C). Interestingly, mice exposed to air puffs responded to ambiguous odor mixtures with fewer licks during the anticipatory odor and delay period indicating that exposure to punishments biased decisions about

178 ambiguous outcomes toward avoidance and away from
 179 approach (Figure 1D). Accordingly, a 2-factor ANOVA
 180 (cue × group) comparing licking rates during cue presen-
 181 tation and delay period in test days demonstrated a sig-
 182 nificant interaction between cue and group ($F_{1,4} = 5.32$,
 183 $p < 0.01$). Notably, the reduced licking to ambiguous
 184 cues in the air puff group was evident on the first trial
 185 of the probe test and persisted throughout all probe test
 186 trials (Figure 1E). Thus, the decline in responding was
 187 not due to effects of extinction in the probe test. In-
 188 deed, both groups showed similar extinction of respond-
 189 ing to ambiguous cues across trials resulting from out-
 190 come omission. Accordingly, a three-factor ANOVA (cue
 191 × trial × group) revealed a significant interaction be-
 192 tween cue and trial ($F_{1,14} = 5.33$, $p < 0.01$). Impor-
 193 tantly, the interaction between cue, group and trial was
 194 not significant ($F_{1,14} = 1.21$, $p = 0.27$).

195 **Punishment history modulates mPFC neuronal
 196 responses to motivationally-relevant stimuli.** Me-
 197 dial PFC (mPFC; also referred to as prelimbic cor-
 198 tex) is known to be involved in learning (Holland and
 199 Gallagher, 2004; Luk and Wallis, 2009; Alexander and
 200 Brown, 2011; Del Arco et al., 2017; Otis et al., 2017;
 201 Orsini et al., 2018), stress (Wellman, 2001; Cook and
 202 Wellman, 2004; Radley et al., 2004, 2005; Liston et al.,
 203 2006; Radley et al., 2006; Cerqueira et al., 2007; Wei
 204 et al., 2007; Liu and Aghajanian, 2008; Radley et al.,
 205 2008; Goldwater et al., 2009; Yuen et al., 2012; Adhikari
 206 et al., 2015), and uncertainty (Ernst and Paulus, 2005;
 207 Opris and Bruce, 2005; Sugrue et al., 2005; Bach et al.,
 208 2009; Levy et al., 2010; Orsini et al., 2018). These func-
 209 tions are critical for making predictions about previously
 210 unobserved stimuli. Such predictions derive from prior
 211 knowledge, as well as experience with the context of an
 212 environment. We thus asked whether mPFC neurons re-
 213 sponded differently to motivationally-relevant stimuli in
 214 the presence or absence of punishment history.

215 We recorded action potentials extracellularly from
 216 2,208 mPFC neurons in 12 mice, 5 exposed to air puffs
 217 (929 neurons), 7 unexposed (1,279 neurons), while mice
 218 performed the go/no-go discrimination task (Supple-
 219 mentary Fig. 1). Most neurons showed firing rate in-
 220 creases or decreases following odor cues, largely with
 221 persistent activity that lasted beyond cue offset. In
 222 particular, to characterize the responses of the popula-
 223 tion, we measured the temporal response profile of each
 224 neuron during sucrose trials by quantifying firing rate
 225 changes from denatonium trials in 100-ms bins using a
 226 receiver operating characteristic (ROC) analysis (Figure
 227 2A). We calculated the area under the ROC curve (au-

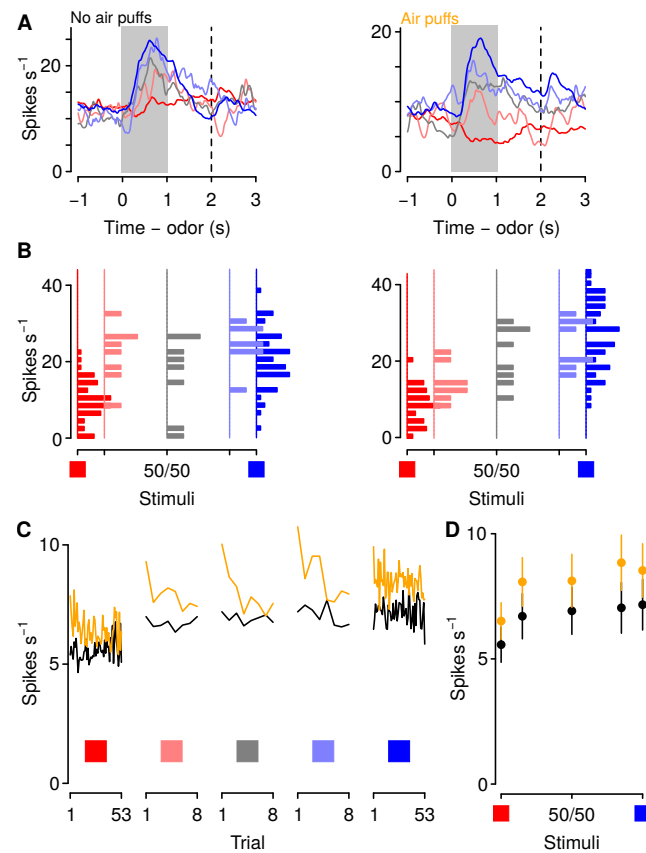


Fig. 3 | Punishment history increases mPFC firing rates to motivationally-relevant cues. (A) Average firing rates from example neurons in a mouse unexposed (left) and exposed (right) to air puffs. Red: denatonium trials. Blue: sucrose trials. Graded colors indicate mixtures as in Fig. 1A. Gray bars indicate a period of odor presentation. Dashed lines indicate outcome delivery. (B) Firing rates for the two example neurons in Fig. 3A during odor and delay period. (C) Trial-by-trial firing rates during sucrose (blue square) and denatonium (red square) trials and during the eight probe trials for each ambiguous cue (light red, gray, light blue squares) for no air puff (black) and air puff (orange) groups, during odor and delay period. (D) Mean \pm SEM firing rates during sucrose (blue square) and denatonium (red square) trials and during the eight probe trials for no air puff (black) and air puff (orange) groups, during odor and delay period.

228 ROC), comparing sucrose trials to denatonium trials.
 229 This analysis determines to what extent an ideal ob-
 230 server could discriminate between activities on the two
 231 trial types. Values of 0.5 indicate no discriminability,
 232 whereas values of 0 or 1 indicate perfect discriminability.
 233 A large fraction of neurons (270 of 929 in mice exposed
 234 to air puffs and 325 of 1,279 in mice unexposed) showed
 235 auROC values greater than 0.7, indicating substantially
 236 greater activity for sucrose compared to denatonium
 237 trials, or values less than 0.3, indicating substantially
 238 greater activity for denatonium compared to sucrose tri-
 239 als (Figure 2A). These patterns were observed in mice

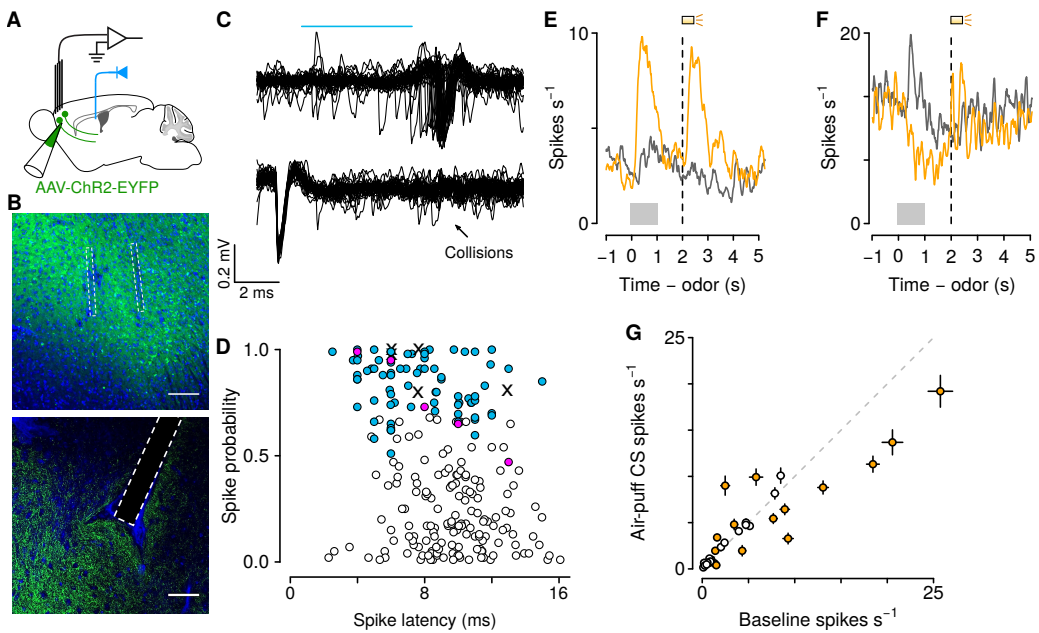


Fig. 4 | Air puff-predicting stimuli modulate mPFC→PVT neuron firing rates. (A) Schematic drawings of viral stereotaxic injection of AAV1-CaMKII-ChR2-eYFP and tetrode bundle into mPFC and optic fiber over PVT. (B) eYFP (green), and DAPI (blue) in mPFC (top) and PVT (bottom) coronal sections from BL6 mice that received AAV1-CaMKII-ChR2-eYFP and tetrode bundle into mPFC and an optic fiber over PVT (scale bar, 100 μ m). (C) Example of an identified corticothalamic neuron responding to a sequence of light stimuli (cyan) with action potentials (top) but not when the light stimuli followed spontaneous action potentials (bottom). (D) Antidromically-tagged corticothalamic neurons (blue) and antidromically-tagged corticothalamic neurons that passed collision tests (magenta). White points are neurons that were not identified. Crosses are neurons that passed collision tests, but were not recorded during behavior. (E-F) Average firing rates from example mPFC→PVT neurons showing firing rate increase (E) or decrease (F) to the air puff-predicting cue. Orange: air puff trials. Gray: CS- trials. Gray bars indicate a period of odor presentation. Dashed lines indicate outcome delivery. (G) Scatter plot showing relationship between the change in neural activity to the air puff-predicting cue compared to baseline firing activity. Orange: neurons in which the firing rate during the air puff-predicting cue was significantly different from baseline firing activity (*t*-test, $p < 0.05$).

exposed and unexposed to air puffs (Figure 2B). Neurons from mice exposed to air puffs responded robustly to both air puff-predicting cues and the air puffs themselves (Figure 2C; Wilcoxon rank sum test, $p < 0.0001$).

We next asked whether a history of air puffs changed the responses of mPFC neurons to aversion- and reward-predictive cues together with ambiguous stimuli. We recorded from 136 neurons from mPFC in the no air puff group and 106 neurons from mPFC in air puff exposed mice during the probe sessions (Figure 3). These populations included 37 in the no air puff group and 25 in the air puff trained group that exhibited auROC discrimination between sucrose and denatonium trials greater than 0.7 or less than 0.3 during the probe sessions. To compare firing rates of those neurons between mice exposed or unexposed to air puffs, we calculated a generalized linear model (Poisson regression) to predict spike counts during the cues as a function of air puff exposure and odor type. Cue-evoked firing rates were significantly higher in mice exposed to air puffs (Figures 3C and 3D; odor mixture $z = 0.18 \pm 0.015$, air-

puff group $z = 0.043 \pm 0.014$, stimulus-group interaction $z = 0.033 \pm 0.019$, $p < 0.001$).

Punishment history modulates corticothalamic neuronal responses to motivationally-significant stimuli.

The neural data described above suggests that a subgroup of mPFC neurons is modulated by punishment history. One of the major projection targets of the mPFC is the paraventricular nucleus of the thalamus (mPFC→PVT). Studies examining the role of PVT in regulating behavioral responses have found that PVT neurons are activated by cues or contexts previously associated with positive or negative emotional outcomes (Beck and Fibiger, 1995; Schiltz et al., 2007; Yasoshima et al., 2007; Choi et al., 2010; Igelstrom et al., 2010; Haight and Flagel, 2014; Hsu et al., 2014; Do-Monte et al., 2015; Kirouac, 2015; Matzeu et al., 2015; Penzo et al., 2015; Li et al., 2016; Zhu et al., 2016; Do-Monte et al., 2017). Additionally, activity in corticothalamic neurons suppresses both the acquisition and expression of conditioned reward seeking Otis et al. (2017). Thus, we hypothesized that mPFC→PVT neurons encode in-

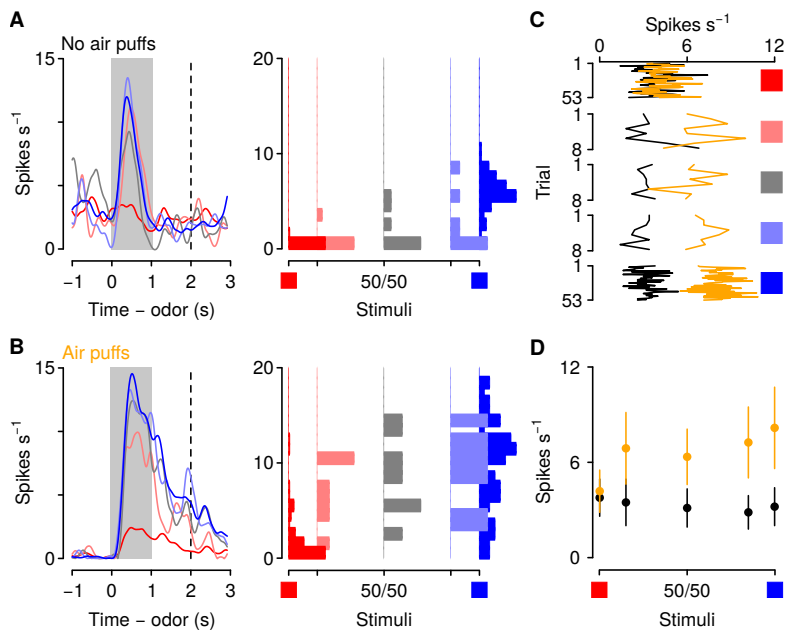


Fig. 5 | Punishment history increases corticothalamic firing rates to motivationally-relevant cues. (A-B) Average firing rates (left) and firing rates during odor and delay period (right) from example neurons in a mouse unexposed (A) and exposed (B) to air puffs. Red: denatonium trials. Blue: sucrose trials. Graded colors indicate mixtures as in Fig. 1A. Gray bars indicate a period of odor presentation. Dashed lines indicate outcome delivery. (C) Trial-by-trial firing rates during sucrose (blue square) and denatonium (red square) trials and during the eight probe trials for each ambiguous cue (light red, gray, light blue squares) for no air puff (black) and air puff (orange) groups, during odor and delay period. (D) Mean \pm SEM firing rates during sucrose (blue square) and denatonium (red square) trials and during the eight probe trials for no air puff (black) and air puff (orange) groups, during odor and delay period.

formation about appetitive and aversive stimuli, and that this information is critical for weighing prior experience in those predictions.

To test this hypothesis, we performed projection-specific electrophysiological recordings from mPFC→PVT neurons while mice performed the go/no-go task. We expressed the light-gated ion channel channelrhodopsin-2 (ChR2, using adeno-associated viruses, AAV1-CaMKIIa-ChR2-eYFP) in pyramidal neurons of the mPFC and we implanted an optic fiber above the PVT, to activate mPFC→PVT cells antidromically (Figure 4A, B). Virus expression and optic fiber implantation were verified histologically (Supplementary Figure 2). At the end of each recording session, we used ChR2 excitation to observe antidromically-evoked spikes. For each neuron, we measured the response to light stimulation and the shape of spontaneous spikes (Figure 4C). To unequivocally identify mPFC→PVT neurons, ChR2-expressing cells in the mPFC were identified with axonal photostimulation and extracellular recordings in mPFC using a collision test (Figure 4D; Paintal, 1959; Bishop et al., 1962; Darian-Smith et al., 1963). Based on the parameters of cells that passed the collision test, we only included units that responded to light with a latency less than

15 ms and spiked in response to at least 70% of all pulses (in response to 10 Hz pulses; Figure 4D). These criteria are comparable to the fastest responses seen using antidromic stimulation with collision tests in corticothalamic neurons in sensory regions of neocortex (Swadlow and Weyand, 1981; Swadlow, 1998; Stoelzel et al., 2017).

We identified 39 and 45 neurons as projecting to PVT in mice unexposed and exposed to air puffs, respectively (Figure 4D; no air puff group: 18 and 21 neurons during conditioning and probe sessions, respectively; air puff group: 35 and 10 neurons during conditioning and probe sessions, respectively). We first asked whether these neurons responded to aversive stimuli. Previous studies have emphasized the role of the PVT in shaping behavioral responses to stimuli that predict aversive outcomes (Beck and Fibiger, 1995; Yasoshima et al., 2007; Hsu et al., 2014; Do-Monte et al., 2015; Penzo et al., 2015), but it's unknown which of its inputs may drive those responses. We found that 43% of mPFC→PVT neurons recorded from mice in the air puff group showed firing rate changes (increases or decreases) in response to air-puff-predicting stimuli (Figures 4E-G). This demonstrates that mPFC→PVT neurons, thought to be involved in behavioral responses to aversive-predicting

332 stimuli, are indeed modulated by those stimuli.

333 We next compared the responses of mPFC→PVT neu-
 334 rons to sucrose- and denatonium-predictive cues and
 335 ambiguous stimuli. In both groups, firing rates of
 336 mPFC→PVT neurons for odor mixtures scaled with
 337 the proportion of the mixture that was the sucrose-
 338 predicting odor, indicating that corticothalamic neurons
 339 responded to parametrically varying ambiguous stim-
 340 ulti with smoothly varying neural responses (Figure 5A-
 341 B). Interestingly, corticothalamic neurons from mice ex-
 342 posed to air puffs responded to the sucrose-predictive cue
 343 and ambiguous odor mixtures with higher phasic activ-
 344 ity during the anticipatory odor and delay period, in-
 345 dicating that exposure to punishments biases neural re-
 346 sponses of corticothalamic neurons to reward-predictive
 347 and ambiguous stimuli (Figure 5C-D; Poisson regression,
 348 odor mixture $z = 0.26 \pm 0.10$, $p < 0.01$, air-puff group
 349 $z = 0.73 \pm 0.15$, $p < 0.01$, stimulus-group interaction
 350 $z = 0.27 \pm 0.22$, $p > 0.2$).

351 Excitation of corticothalamic neurons modulates 352 behavioral responses to motivationally-relevant 353 cues.

354 The neural data described above suggests that
 355 elevated activity in corticothalamic neurons to the
 356 aversion- and reward-predictive cues together with the
 357 ambiguous cues is critical for modulating behavioral re-
 358 sponse to those stimuli. To provide a more specific test
 359 of this hypothesis, we next used optogenetic methods to
 360 activate corticothalamic neurons selectively at the time
 361 of presentation of those cues in mice trained in the same
 362 go/no-go task described above but with no exposure
 363 to air puffs. Mice received bilateral infusions of either
 364 AAV1/5-CaMKIIa-ChR2-eYFP or AAV1/5-CaMKIIa-
 365 eYFP (control) into mPFC; expression was verified his-
 366 tologically (Supplementary Figure 3). Mice also received
 367 fiber optic implants over PVT (Figure 6A). Three weeks
 368 after surgery, these mice began training in the go/no-go
 369 discrimination task and, during the probe session, light
 370 was delivered into the PVT in 5 random trials of all su-
 371 crose and denatonium trials and in half of all the ambigu-
 372 ous trials, in the cue and delay period (Figure 6B). We
 373 used a 10 Hz frequency stimulation because it resembled
 374 the firing rate of corticothalamic neurons in response to
 375 ambiguous stimuli observed in neural recordings; we also
 376 used a 20 Hz frequency in order to get a frequency re-
 377 sponse curve. All mice underwent conditioning sessions
 378 and there were neither main effects nor any interactions
 379 of group on conditioned responding across conditioning
 380 ($F < 1.14$; $p > 0.33$) (Figure 6C). During the subsequent
 381 probe test, ChR2 mice showed a reduction in response
 382 to denatonium- and sucrose-predictive cues and ambigu-
 383 ous cues in the trials in which light was delivered in a
 384 frequency-dependent manner, whereas eYFP mice that
 385 received the same treatment responded equally in trials
 386 with or without light delivery (Figure 6D-E). Accord-

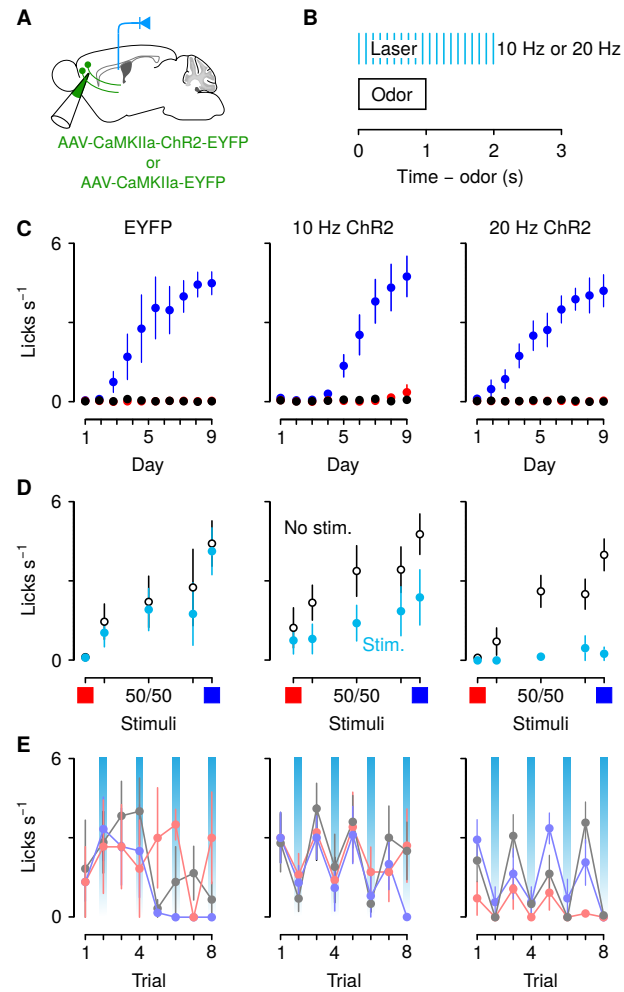


Fig. 6 | Optogenetic excitation of corticothalamic neurons negatively biases responses to motivationally-relevant stimuli. (A) Schematic of viral stereotaxic injection of AAV1/5-CaMKIIa-ChR2-eYFP or AAV1/5-CaMKIIa-eYFP into mPFC and optic fiber over PVT. (B) Optical stimulation was delivered during presentation of the cue and during the 1 s delay before outcome delivery. (C) Licking rates in eYFP (left, $n = 3$), 10 Hz ChR2-eYFP (center, $n = 5$), and 20 Hz ChR2-eYFP (right, $n = 7$) groups across conditioning, during odor and delay period, for sucrose (blue), denatonium (red), and no-outcome (black) trials. (D) Licking rates during sucrose (red square) and denatonium (blue square) trials and during the eight probe trials (light blue, gray and light red squares) for eYFP (left), 10 Hz ChR2-eYFP (center) and 20 Hz ChR2-eYFP (right) groups, during odor and delay period, with (light blue) or without (white) laser stimulation. (E) Trial-by-trial licking rates during 85%A/15%B (light red), 50%A/50%B (gray), 15%A/85%B (light blue) trials for eYFP (left), 10 Hz ChR2-eYFP (center) and 20 Hz ChR2-eYFP (right) groups, during odor and delay period, with (light blue shadows) or without laser stimulation. Line and error bars represent the mean \pm SEM.

ous cues in the trials in which light was delivered in a frequency-dependent manner, whereas eYFP mice that received the same treatment responded equally in trials with or without light delivery (Figure 6D-E). Accord-

386 ingly, a 3-factor ANOVA (cue × stimulation × group)
387 comparing licking behavior during cue presentation and
388 delay period in stimulated versus unstimulated trials in
389 eYFP, 10 Hz and 20 Hz groups revealed a significant
390 main effect of cue ($F_{1,4} = 13.8, p < 0.01$) and stimulation
391 ($F_{1,1} = 30.11, p < 0.01$). Moreover, there was a sig-
392 nificant interaction between cue and group ($F_{1,8} = 4.8,$
393 $p < 0.01$) and stimulation and group ($F_{1,2} = 4.68,$
394 $p < 0.05$).

395 Stimulation of the same neurons did not, however, dis-
396 rupt licking for an unpredictable reward. Outside of the
397 task, we delivered randomly-timed sucrose rewards (3
398 μl). Mice licked at high rates to consume unexpected
399 rewards (Supplementary Figure 4). Importantly, stim-
400 ulation of mPFC→PVT axons during reward delivery
401 at the same frequencies used in the behavioral task in
402 half of the total number of trials did not change the num-
403 ber of licks in response to these rewards (Supplementary
404 Figure 4). Accordingly, a 2-factor ANOVA (frequency of
405 stimulation × group) comparing licking behavior during
406 stimulated and unstimulated trials revealed no signifi-
407 cant main effect or interaction with group (all $F < 0.23,$
408 $p > 0.65$). Thus, uncued licking is not altered by opto-
409 genetic excitation of mPFC→PVT cells and the optoge-
410 netic effects are not due to a light-induced impairment
411 in licking in general.

412 Discussion

413 In this study, we examined the projection from mPFC to
414 PVT in mice approaching or avoiding negative and pos-
415 itive valence-predictive stimuli. We found that a history
416 of punishments negatively biased behavioral responses
417 to those motivationally-relevant stimuli while selec-
418 tively increasing excitatory responses of PVT-projecting
419 mPFC neurons. Indeed, mice exposed to punishments
420 showed reduced approach behavior to reward-predictive
421 and ambiguous stimuli than mice unexposed to punish-
422 ments. Moreover, artificially increasing activity from
423 mPFC to PVT quantitatively mimicked the punishment-
424 induced negative behavioral bias.

425 Cognitive processes—appraisals of stimuli, events and
426 situations—play an important role in generating affec-
427 tive states, and vice versa, these affective states influence
428 cognitive functioning by inducing attentional, memory,
429 and judgment biases (Lerner and Keltner, 2000; Hasel-
430 ton et al., 2009; Harding et al., 2004; Enkel et al., 2010;
431 Rygula et al., 2012; Papciak et al., 2013; Rygula et al.,
432 2013; Parker et al., 2014; Rygula et al., 2014). Among
433 brain regions that are engaged in affective processing,
434 the mPFC has long been implicated in adaptive respond-

435 ing by signaling information about expected outcome
436 and by regulating sensitivity to reward and punishment
437 (Holland and Gallagher, 2004; Luk and Wallis, 2009;
438 Alexander and Brown, 2011; Del Arco et al., 2017; Orsini
439 et al., 2018). Here, we found that firing rates in mPFC
440 neurons reflect cue-evoked expectations for aversion- and
441 reward-predictive cues and were enhanced in mice ex-
442 posed to a mild punishment, which correlates with a
443 reduction in anticipatory responses to the same stimuli.
444 Those findings are consistent with a negative bias and
445 suggests that negative events can bias decisions by al-
446 tering the activity of mPFC neurons. Several studies
447 have implicated the prefrontal network in the patho-
448 physiology of affective disorders (Phillips et al., 2003;
449 Drevets et al., 2008) and chronic stress—a crucial factor
450 in increasing the risk of developing affective disorders—
451 has profound detrimental effects on the anatomy and
452 physiology of mPFC neurons (Wellman, 2001; Cook and
453 Wellman, 2004; Radley et al., 2004, 2005; Liston et al.,
454 2006; Radley et al., 2006; Cerqueira et al., 2007; Wei
455 et al., 2007; Liu and Aghajanian, 2008; Radley et al.,
456 2008; Goldwater et al., 2009; Yuen et al., 2012; Adhikari
457 et al., 2015). In particular, chronic stress induces sig-
458 nificant regression of the apical dendrites of pyramidal
459 neurons in mPFC (Cook and Wellman, 2004; Radley
460 et al., 2004; Liston et al., 2006; Goldwater et al., 2009),
461 which may in turn impact mPFC function.

462 The mPFC densely projects to subcortical moti-
463 vationally relevant processing structures, including
464 PVT, amygdala, hippocampus and nucleus accumbens
465 (Vertes, 2004; Li and Kirouac, 2012). Among all brain
466 regions that receive strong projections from the mPFC,
467 PVT has long been considered a stress detector and
468 implicated in the emergence of adaptive responding to
469 stress (Chastrette et al., 1991; Sharp et al., 1991; Cul-
470 linan et al., 1995; Bubser and Deutch, 1999; Spencer
471 et al., 2004; Hsu et al., 2014; Do-Monte et al., 2015;
472 Penzo et al., 2015; Zhu et al., 2016; Do-Monte et al.,
473 2017; Beas et al., 2018; Choi et al., 2019). On the other
474 hand, PVT has also been considered a potential me-
475 diator of motivated behavior responding to both food-
476 and drug-associated cues (Schiltz et al., 2005; Igelstrom
477 et al., 2010; Martin-Fardon and Boutrel, 2012; James
478 and Dayas, 2013; Browning et al., 2014; Haight and
479 Flagel, 2014; Li et al., 2016). Consistent with these
480 findings that put PVT in a unique position to inte-
481 grate information about positive and negative motiva-
482 tionally relevant cues and translate it into adaptive be-
483 havioral responses, we found that mPFC neurons pro-
484 jecting to the PVT maintain cue-evoked expectations for

485 motivationally-relevant outcomes and their neural ac-
486 tivity was enhanced in mice exposed to punishments.
487 Moreover, by mimicking this punishment-induced in-
488 crease of PVT-projecting mPFC neuronal activity with
489 a selectively optogenetic activation of this pathway, we
490 observed a reduction in anticipatory responses to the
491 predictive cues. These findings suggest that informa-
492 tion about cue interpretation is transferred from mPFC
493 to PVT and this pathway is crucial for an adaptive re-
494 sponding toward those stimuli as a function of previous
495 experiences. These results are also consistent with a re-
496 cent study showing that activity in mPFC neurons pro-
497 jecting to the PVT suppresses both the acquisition and
498 expression of conditioned reward seeking (Otis et al.,
499 2017). Based on recent evidence showing two geneti-
500 cally, anatomically and functionally distinct cell types
501 across the anteroposterior axis of the PVT (Gao et al.,
502 2020), it will be interesting to investigate in future stud-
503 ies whether the information from mPFC is transferred
504 to anatomically or molecularly segregated cell types or
505 projection-specific neurons within the PVT.

506 Understanding the underlying mechanisms by which
507 information of cue interpretation is updated as a func-
508 tion of prior experience in the mPFC→PVT circuit is
509 crucial for delving deeper into the brain's neuronal con-
510 nectionality underlying cognitive bias behaviors. Impor-
511 tantly, proper tuning of this network has been shown
512 to be exerted by robust neuromodulation from ascen-
513 ding catecholaminergic systems (Arnsten et al., 2012) and
514 maladaptive processing of these systems has been impli-
515 cated in cognitive deficits associated with several affec-
516 tive disorders (Enkel et al., 2010; Kukolja et al., 2008).
517 For example, acute pharmacological stimulation of the
518 serotonergic and dopaminergic systems has been shown
519 to influence cognitive bias in rodents (Rygula et al.,
520 2014). In particular, citalopram, a selective serotonin
521 reuptake inhibitor, and amphetamine, a powerful psy-
522 chostimulant, both induced a positive cognitive process-
523 ing bias (Rygula et al., 2014). Those results are impor-
524 tant from a clinical point of view, knowing that negative
525 cognitive bias lies at the core of the pathophysiology of
526 several affective disorders and it has been extensively
527 studied in humans (Wright and Bower, 1992; MacLeod
528 and Byrne, 1996; Beck, 2008). For example, it has
529 been shown that patients with anxiety and depression
530 interpret ambiguous information with a negative bias
531 (Schwarz and Clore, 1983; Eysenck et al., 1987; Wright
532 and Bower, 1992; MacLeod and Byrne, 1996; Lawson
533 et al., 2002; Beck, 2008; Chan et al., 2008; Pizzagalli
534 et al., 2008; Dearing and Gotlib, 2009). Thus, yield-

535 ing a clearer vision of how cognitive biases develop and
536 act in several chronic and debilitating neuropsychiatric
537 disorders may offer an unprecedented opportunity for
538 designing novel treatments, aimed at ameliorating the
539 proper functional tuning and connectivity of prefrontal-
540 orchestrated neuronal circuits.

541 In summary, by means of a mild punishment we in-
542 duced a negative bias in mice which was linked to a hy-
543 peractivity in neural responses of PVT-projecting mPFC
544 neurons. Artificial activation of the same pathway re-
545 capitulated the behavioral outcome. Thus, our results
546 highlight a fundamental role for the mPFC→PVT cir-
547 cuit in shaping adaptive responses by modulating predic-
548 tions about imminent motivationally-relevant outcomes
549 as a function of prior experience.

550 Materials and methods

551 **Subjects.** Wild-type C57BL/6J male mice (The Jack-
552 son Laboratory, 000664), 8-10 weeks old at the time of
553 surgery, were housed in a reverse 12-hour light-dark cy-
554 cle room (lights on at 20:00). All mice were given ad
555 libitum water except during testing periods. During be-
556 havioral testing, mice were water deprived by giving 1ml
557 of water per day. Food was freely available throughout
558 the experiments. All testing was conducted in accord-
559 ance with the National Institutes of Health Guide for
560 the Care and Use of Laboratory Animals and approved
561 by the Johns Hopkins University Animal Care and Use
562 Committee.

563 **Stereotaxic surgeries.** All mice were surgically im-
564 planted with custom-made titanium head plates using
565 dental adhesive (C&B-Metabond, Parkell) under isoflu-
566 rane anesthesia (1.0-1.5% in O₂). Surgeries were con-
567 ducted under aseptic conditions and analgesia (ketopro-
568 fen, 5 mg/kg and buprenorphine, 0.05-0.1 mg/kg) was
569 administered postoperatively. Mice recovered for 7-10
570 days before starting behavioral testing.

571 For electrophysiological experiments, we implanted
572 unilaterally a custom microdrive containing 8 drivable
573 tetrodes made from nichrome wire (PX000004, Sandvik)
574 and positioned inside 39 ga polyimide guide tubes. We
575 targeted mPFC under stereotaxic guidance at 2.2 mm
576 anterior and 0.4 mm lateral to bregma and 1.6 mm ven-
577 tral to the skull. Tetrodes were advanced subsequently
578 into final positions in mPFC during recording. For iden-
579 tifying corticothalamic neurons, an optic fiber was im-
580 planted over PVT under stereotaxic guidance at 1.4 mm
581 anterior and 1.3 mm lateral to bregma and 3.6 mm ven-
582 tral to the skull with a 22.5° angle.

583 For optogenetic experiments, AAV1/5-CamKIIa-
584 hChR2(H134R)-eYFP or AAV1/5-CamKIIa-eYFP
585 (AAV5: from UNC GTC Vectore Core; AAV1: from
586 Addgene) was injected bilaterally in mPFC under
587 stereotaxic guidance at 2.2 mm anterior and 0.3 mm
588 lateral to bregma and 1.6 mm ventral to the skull.
589 pAAV-CaMKIIa-hChR2(H134R)-EYFP was a gift from
590 Karl Deisseroth (Addgene viral prep 26969-AAV1;
591 <http://n2t.net/addgene:26969>; RRID:Addgene_26969)
592 (Lee et al., 2010). A total of 300 nl of virus (titer
593 $\sim 10^{13}$ GC/mL) per hemisphere was delivered at the
594 rate of 1 nl/s (MMO-220A, Narishige). The injection
595 pipette was left in place for 5 min after each injection.
596 Optic fibers (200 μ m diameter, 0.39 NA, Thorlabs) were
597 implanted bilaterally over mPFC (at 2.2 mm anterior
598 and 0.6 mm lateral to bregma and 1.3 mm ventral to
599 the skull with a 10° angle) or unilaterally over PVT (at
600 1.4 mm anterior and 1.3 mm lateral to bregma and 3.6
601 mm ventral to the skull with a 22.5° angle).

602 **Behavioral task.** Following recovery from surgery,
603 water-restricted mice were habituated for 3 days while
604 head-fixed before training on the go/no-go task. Each
605 mouse performed behavioral tasks at the same time of
606 day (between 08:00 a.m. and 2:00 p.m.). All behavioral
607 tasks were performed in dark, sound-attenuated cham-
608 ber, with white noise delivered between 2-60 kHz (L60
609 Ultrasound Speaker, Pettersson). Odors were delivered
610 with a custom-made olfactometer (Cohen et al., 2012).
611 Each odor was dissolved in mineral oil at 1:10 dilution.
612 Diluted odors (30 μ l) were placed on filter-paper housing
613 (Whatman, 2.7 μ m pore size). Odorized air was further
614 diluted with filtered air by 1:10 to produce a 1.0 l/min
615 flow rate. Licks were detected by charging a capacitor
616 (MPR121QR2, Freescale). Task events were controlled
617 with a microcontroller (ATmega16U2 or ATmega328).
618 Reinforcements were 3 μ l of sucrose (an appetitive sweet
619 solution), denatonium (an aversive bitter solution) or air
620 puff (40 psi), delivered using solenoids (LHDA1233115H,
621 The Lee Co). Intertrial intervals (ITIs) were drawn from
622 an exponential distribution with a rate parameter of 0.3,
623 with a maximum of 30 s. This resulted in a flat ITI haz-
624 ard function, ensuring that expectation about the start
625 of the next trial did not increase over time (Luce, 1986).
626 The mean ITI was 7.2 s (range 2.4-30.0 s).

627 Mice underwent 10 conditioning sessions. In each ses-
628 sion, mice received 50 1-s presentations of four different
629 olfactory stimuli (A, B, C, and D). The order of odor
630 presentations was randomized among mice and among
631 sessions. For all conditioning, A, B, C, and D con-
632 sisted of (+)-limonene, p-cymene, pentylacetate, and

acetophenone, respectively (counterbalanced). 1-s after
633 termination of A, sucrose was delivered and 1-s after ter-
634mination of B, denatonium was delivered. C was paired
635 with no reinforcement. In the air puff group, 1-s after
636 termination of D, an unavoidable air puff was delivered
637 to their right eye, while in the control group, D was
638 paired with no reinforcement. 4-s after the presentation
639 of each odor, a vacuum was activated to remove any
640 residual of sucrose or denatonium. After the activation
641 of the vacuum, there was a fixed 3 second delay and then
642 the variable ITI will follow. After completion of condi-
643 tioning training, mice received a single extinction probe
644 session. During the probe session, the 4 conditioning
645 odors were continued to be presented (53 trials for each
646 odor), but mice also received eight non-reinforced pres-
647 entations of three mixtures of varying proportions of A
648 and B odors: 85%A/15%B, 50%A/50%B, 15%A/85%B.
649 These odor mixture trials were interleaved with the 4
650 conditioning odor trials in a randomized order.
651

In mice designated for the mPFC electrophysiological
652 experiments, following the probe test, mice underwent
653 reversal learning, in which A and B were reversed. 1 s
654 after termination of A, denatonium was delivered and
655 1 s after termination of B, sucrose was delivered. C
656 and D were continued to be presented as in condi-
657 tioning. Then, mice received another single extinction probe
658 session, identical to the one received after conditioning.
659 Neural data from the initial extinction days were not sta-
660 tistically different from data gathered in later rounds of
661 training and thus these neurons were analyzed together
662 in the text.

In mice designated for the PVT-projecting mPFC
663 electrophysiological experiments, following the probe
664 test, mice repeated three days of conditioning and then
665 underwent additional rounds of probe test days in order
666 to acquire additional data. This was done up to
667 three times for a given mouse. Neural data from the ini-
668 tial extinction days were not statistically different from
669 data gathered in later rounds of training and thus these
670 neurons were analyzed together in the text.
671

In mice designated for the optogenetic experiments,
672 training began approximately 3 weeks after viral injec-
673 tion and fiber implantation, and light (473 nm, 10-12
674 mW) was delivered into the PVT during the probe ses-
675 sion. During the behavioral task, light was delivered in
676 half of all the ambiguous trials, during the cue and delay
677 epoch. Moreover, light was also delivered in 5 random
678 trials of all sucrose and denatonium trials, during the cue
679 and delay epoch. The primary measure of conditioning
680 to cues was the number of licks during odor presenta-
681 tion.

683 and the second preceding reinforcement delivery. During
684 the un-cued stimulation trials, light was delivered in half
685 of all trials, during the presentation of reward delivery
686 and lasted for 1500 ms.

687 **Electrophysiology.** Throughout the discrimination
688 task, mice were attached to the recording cable and before
689 each session, tetrodes were screened for activity. Active
690 tetrodes were selected for recording, and the session
691 was begun. On the rare occasion that fewer than 4 of
692 8 tetrodes had single units, the tetrode assembly was
693 advanced 40 or 80 μm at the end of the session. Otherwise,
694 the tetrode assembly was kept in the same position
695 between sessions until the probe test day. After the ex-
696 tinction probe test, the tetrode assembly was advanced
697 80 μm regardless of the number of active tetrodes in order
698 to acquire activity from a new group of neurons in
699 any subsequent training.

700 We recorded extracellularly (Digital Lynx 4SX, Neuralynx Inc.) from multiple neurons simultaneously at 32
701 kHz using custom-built screw-driven microdrives with 8
702 tetrodes coupled to a 200 μm fiber optic (32 channels
703 total). All tetrodes were gold-plated to an impedance of
704 200–300 $\text{k}\Omega$ prior to implantation. Spikes were bandpass
705 filtered between 0.3–6 kHz and sorted online and offline
706 using Spikesort 3D (Neuralynx Inc.) and custom soft-
707 ware written in MATLAB. To measure isolation quality
708 of individual units, we calculated the L-ratio (Schmitzer-
709 Torbert et al., 2005) and fraction of interspike interval
710 (ISI) violations within a 2 ms refractory period. All sin-
711 gular units included in the dataset had an L-ratio less than
712 0.05 and less than 0.1% ISI violations. We only included
713 units that had a firing rate of greater than 0.5 spikes s^{-1}
714 over the course of the recording session.

716 **Optogenetic identification.** To verify that our
717 recordings targeted corticothalamic neurons, at the end
718 of daily recording sessions, we used channelrhodopsin ex-
719 citation to observe stimulation-locked spikes, by deliv-
720 ering 3–5 ms pulses of 473 nm light at 15 mW using
721 a diode-pumped solid-state laser (Laserglow), together
722 with a shutter (Uniblitz). Spike shape was measured
723 using a broadband signal (0.1 Hz–9 kHz) sampled at 32
724 kHz. This ensured that particular features of the spike
725 waveform were not missed. We delivered 10 trains of
726 light (10 pulses per train, 10 s between trains) at 10 Hz,
727 resulting in 100 total pulses. For collision tests, we de-
728 livered light over PVT (2 ms pulse, 473 nm, 15 mW)
729 triggered by a spontaneous action potential. Identified
730 neurons did not show stimulus-locked spikes following
731 spontaneous spikes (“collisions”).

732 **Histology.** At the end of behavioral testing, all mice

733 were deeply anesthetized and then transcardially per-
734 fused with 4% paraformaldehyde (wt/vol). The brains
735 were removed and processed for histology using standard
736 techniques. For the electrophysiological experiments, we
737 verified recording sites histologically with electrolytic le-
738 sions (15 s of 10 μA direct current across two wires of
739 the same tetrode). For optogenetic experiments, virus
740 expression was examined using a confocal microscope
741 (Zeiss LSM 800). After histological verification, mice
742 with incorrect virus injection or tetrode implantation
743 were excluded from data analysis.

744 **Data analysis.** All analyses were performed
745 with MATLAB (Mathworks) and R (<http://www.r-project.org/>). All data are presented as mean \pm SEM
746 unless reported otherwise. All statistical tests were two-
747 sided. For nonparametric tests, the Wilcoxon rank-sum
748 test was used, unless data were paired, in which case the
749 Wilcoxon signed-rank was used. To estimate neuronal
750 learning rates (Figure 2), we used logistic functions of
751 the form $f(x) = \frac{L}{1+e^{-k(x-x_0)}}$. Learning rates are es-
752 timates of the k parameter.

753 **Acknowledgements** We thank T. Shelley for machin-
754 ing, and G. Schoenbaum, M. Pignatelli, and the Cohen
755 Lab for comments. This work was supported by Life
756 Sciences Research Foundation (F.L.), F30MH110084
757 (B.A.B.), Klingenstein-Simons, MQ, NARSAD, White-
758 hall, R01DA042038, and R01NS104834 (J.Y.C.), and
759 P30NS050274.

762 References

- 763 Adhikari A, Lerner TN, Finkelstein J, Pak S, Jennings
764 JH, Davidson TJ, Ferenczi E, Gunaydin LA, Mirz-
765 abekov JJ, Ye L, Kim SY, Lei A, Deisseroth K. Baso-
766 medial amygdala mediates top-down control of anxi-
767 ety and fear. *Nature* 527: 179–185, 2015.
- 768 Alexander WH, Brown JW. Medial prefrontal cortex as
769 an action-outcome predictor. *Nat Neurosci* 14: 1338–
770 1344, 2011.
- 771 Amemori Ki, Graybiel AM. Localized microstimulation
772 of primate pregenual cingulate cortex induces negative
773 decision-making. *Nat Neurosci* 15: 776–785, 2012.
- 774 Arnsten AFT, Wang MJ, Paspalas CD. Neuromodula-
775 tion of thought: flexibilities and vulnerabilities in
776 prefrontal cortical network synapses. *Neuron* 76: 223–
777 239, 2012.

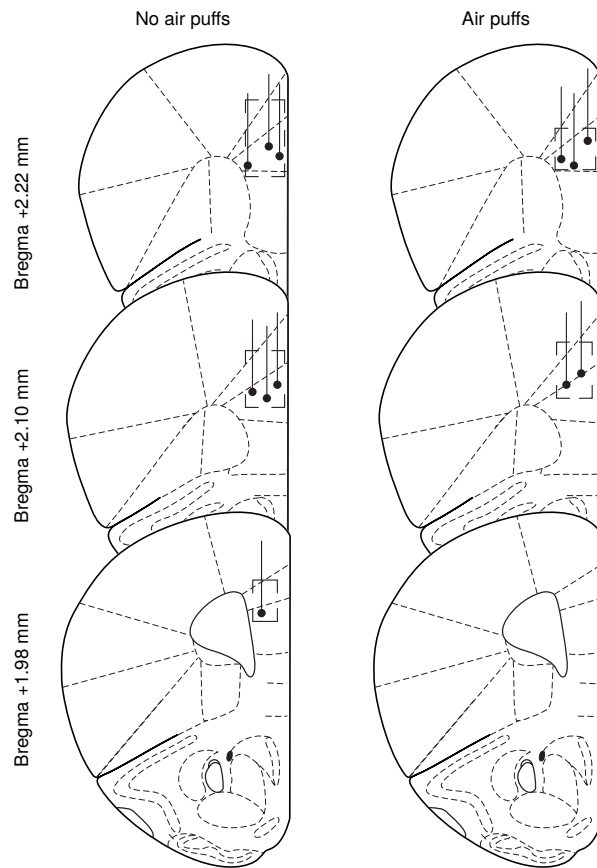
- 778 Bach DR, Seymour B, Dolan RJ. Neural activity associated
779 with the passive prediction of ambiguity and risk
780 for aversive events. *J Neurosci* 29: 1648–1656, 2009.
781 Bari BA, Grossman CD, Lubin EE, Rajagopalan AE,
782 Cressy JI, Cohen JY. Stable representations of decision
783 variables for flexible behavior. *Neuron* 103: 922–
784 933.e7, 2019.
785 Beas BS, Wright BJ, Skirzewski M, Leng Y, Hyun
786 JH, Koita O, Ringelberg N, Kwon HB, Buonanno A,
787 Penzo MA. The locus coeruleus drives disinhibition in
788 the midline thalamus via a dopaminergic mechanism.
789 *Nat Neurosci* 21: 963–973, 2018.
790 Bechara A, Damasio H, Damasio A. Emotion, decision
791 making and the orbitofrontal cortex. *Cereb Cortex* 10:
792 295–307, 2000.
793 Beck AT. The evolution of the cognitive model of depression
794 and its neurobiological correlates. *Am J Psychiatr*
795 165: 969–977, 2008.
796 Beck CH, Fibiger HC. Conditioned fear-induced changes
797 in behavior and in the expression of the immediate
798 early gene c-fos: with and without diazepam pretreatment.
799 *J Neurosci* 15: 709–720, 1995.
800 Bishop P, Burke W, Davis R. Single-unit recording from
801 antidromically activated optic radiation neurones. *J
802 Physiol* 162: 432–450, 1962.
803 Blum S, Runyan JD, Dash PK. Inhibition of prefrontal
804 protein synthesis following recall does not disrupt
805 memory for trace fear conditioning. *BMC Neurosci*
806 7: 67, 2006.
807 Boleij H, van't Klooster J, Lavrijsen M, Kirchhoff S,
808 Arndt SS, Ohl F. A test to identify judgement bias in
809 mice. *Behav Brain Res* 233: 45–54, 2012.
810 Browning JR, Jansen HT, Sorg BA. Inactivation of the
811 paraventricular thalamus abolishes the expression of
812 cocaine conditioned place preference in rats. *Drug
813 Alcohol Depend* 134: 387–390, 2014.
814 Bubser M, Deutch AY. Stress induces Fos expression in
815 neurons of the thalamic paraventricular nucleus that
816 innervate limbic forebrain sites. *Synapse* 32: 13–22,
817 1999.
818 Burgos-Robles A, Bravo-Rivera H, Quirk GJ. Prelimbic
819 and infralimbic neurons signal distinct aspects of appetitive
820 instrumental behavior. *PLoS ONE* 8: e57575,
821 2013.
822 Burgos-Robles A, Kimchi EY, Izadmehr EM, Porzenheim
823 MJ, Ramos-Guasp WA, Nieh EH, Felix-Ortiz
824 AC, Namburi P, Leppla CA, Presbrey KN, Anandalingam
825 KK, Pagan-Rivera PA, Anahtar M, Beyeler
826 A, Tye KM. Amygdala inputs to prefrontal cortex
827 guide behavior amid conflicting cues of reward and
828 punishment. *Nat Neurosci* 20: 824–835, 2017.
829 Burgos-Robles A, Vidal-Gonzalez I, Quirk GJ. Sustained
830 conditioned responses in prelimbic prefrontal
831 neurons are correlated with fear expression and extinction
832 failure. *J Neurosci* 29: 8474–8482, 2009.
833 Cerqueira JJ, Mailliet F, Almeida OFX, Jay TM, Sousa
834 N. The prefrontal cortex as a key target of the maladaptive
835 response to stress. *J Neurosci* 27: 2781–2787,
836 2007.
837 Chan SWY, Harmer CJ, Goodwin GM, Norbury R.
838 Risk for depression is associated with neural biases in
839 emotional categorisation. *Neuropsychologia* 46: 2896–
840 2903, 2008.
841 Chastrette N, Pfaff DW, Gibbs RB. Effects of daytime
842 and nighttime stress on Fos-like immunoreactivity in
843 the paraventricular nucleus of the hypothalamus, the
844 habenula, and the posterior paraventricular nucleus of
845 the thalamus. *Brain Res* 563: 339–344, 1991.
846 Choi DL, Davis JF, Fitzgerald ME, Benoit SC. The role
847 of orexin-A in food motivation, reward-based feeding
848 behavior and food-induced neuronal activation in rats.
849 *Neuroscience* 167: 11–20, 2010.
850 Choi EA, Jean-Richard-dit Bressel P, Clifford CW, Mc-
851 Nally GP. Paraventricular thalamus controls behavior
852 during motivational conflict. *J Neurosci* pp. 2480–18,
853 2019.
854 Cohen JY, Haesler S, Vong L, Lowell BB, Uchida N.
855 Neuron-type-specific signals for reward and punishment
856 in the ventral tegmental area. *Nature* 482: 85–
857 88, 2012.
858 Cook SC, Wellman CL. Chronic stress alters dendritic
859 morphology in rat medial prefrontal cortex. *J Neuro-
860 biol* 60: 236–248, 2004.
861 Corcoran KA, Quirk GJ. Activity in prelimbic cortex is
862 necessary for the expression of learned, but not innate,
863 fears. *J Neurosci* 27: 840–844, 2007.
864 Courtin J, Chaudun F, Rozeske RR, Karalis N,
865 Gonzalez-Campo C, Wurtz H, Abdi A, Baufreton J,
866

- 866 Bienvenu TCM, Herry C. Prefrontal parvalbumin in- 909
867 terneurons shape neuronal activity to drive fear ex- 910
868 pression. *Nature* 505: 92–96, 2014. 911
869 Cullinan WE, Herman JP, Battaglia DF, Akil H, Watson 912
870 SJ. Pattern and time course of immediate early gene 913
871 expression in rat brain following acute stress. *Neuro- 914
872 science* 64: 477–505, 1995. 915
873 Darian-Smith I, Phillips G, Ryan R. Functional organiza- 916
874 tion in the trigeminal main sensory and rostral 917
875 spinal nuclei of the cat. *J Physiol* 168: 129–146, 1963. 918
876 Dearing KF, Gotlib IH. Interpretation of ambiguous 919
877 information in girls at risk for depression. *J Abnorm 920
878 Child Psychol* 37: 79–91, 2009. 921
879 Del Arco A, Park J, Wood J, Kim Y, Moghaddam 922
880 B. Adaptive encoding of outcome prediction by pre- 923
881 frontal cortex ensembles supports behavioral flexibil- 924
882 ity. *J Neurosci* 37: 8363–8373, 2017. 925
883 Deldin PJ, Levin IP. The effect of mood induction in 926
884 a risky decision-making task. *Bull Psychon Soc* 24: 927
885 4–6, 1986. 928
886 Do-Monte FH, Minier-Toribio A, Quiñones-Laracuente 929
887 K, Medina-Coln EM, Quirk GJ. Thalamic Regulation 930
888 of Sucrose Seeking during Unexpected Reward Omis- 931
889 sion. *Neuron* 94: 388–400.e4, 2017. 932
890 Do-Monte FH, Quiñones-Laracuente K, Quirk GJ. A 933
891 temporal shift in the circuits mediating retrieval of 934
892 fear memory. *Nature* 519: 460–463, 2015. 935
893 Dolan R. Emotion, cognition, and behavior. *Science* 936
894 298: 1191–1194, 2002. 937
895 Drevets WC, Price JL, Furey ML. Brain structural and 938
896 functional abnormalities in mood disorders: implications 939
897 for neurocircuitry models of depression. *Brain Struct Funct* 213: 93–118, 2008. 940
898 Enkel T, Gholizadeh D, von Bohlen Und Halbach O, 941
899 Sanchis-Segura C, Hurlemann R, Spanagel R, Gass P, 942
900 Vollmayr B. Ambiguous-cue interpretation is biased 943
901 under stress- and depression-like states in rats. *Neu- 944
902 roropsychopharmacology* 35: 1008–1015, 2010. 945
903 Ernst M, Paulus MP. Neurobiology of decision making: 946
904 a selective review from a neurocognitive and clinical 947
905 perspective. *Biol Psychiat* 58: 597–604, 2005. 948
906 Eysenck MW, MacLeod C, Mathews A. Cognitive func- 949
907 tioning and anxiety. *Psychol Res* 49: 189–195, 1987. 950
908
Gao C, Leng Y, Ma J, Rooke V, Rodriguez-Gonzalez 909
S, Ramakrishnan C, Deisseroth K, Penzo MA. Two 910
genetically, anatomically and functionally distinct cell 911
types segregate across anteroposterior axis of paraven- 912
tricular thalamus. *Nat Neurosci* 23: 217–228, 2020. 913
Goldwater DS, Pavlides C, Hunter RG, Bloss EB, Hof 914
PR, McEwen BS, Morrison JH. Structural and func- 915
tional alterations to rat medial prefrontal cortex fol- 916
lowing chronic restraint stress and recovery. *Neuro- 917
science* 164: 798–808, 2009. 918
Haight JL, Flagel SB. A potential role for the paraven- 919
tricular nucleus of the thalamus in mediating indi- 920
vidual variation in Pavlovian conditioned responses. 921
Front Behav Neurosci 8: 79, 2014. 922
Harding EJ, Paul ES, Mendl M. Animal behaviour: cog- 923
nitive bias and affective state. *Nature* 427: 312, 2004. 924
Haselton MG, Bryant GA, Wilke A, Frederick DA, 925
Galperin A, Frankenhuus WE, Moore T. Adaptive 926
rationality: An evolutionary perspective on cognitive 927
bias. *Soc Cogn* 27: 733–763, 2009. 928
Hockey GRJ, John Maule A, Clough PJ, Bdzola L. Ef- 929
fects of negative mood states on risk in everyday de- 930
cision making. *Cogn Emot* 14: 823–855, 2000. 931
Holland PC, Gallagher M. Amygdala-frontal interac- 932
tions and reward expectancy. *Curr Opin Neurobiol* 933
14: 148–155, 2004. 934
Hsu DT, Kirouac GJ, Zubieta JK, Bhatnagar S. Con- 935
tributions of the paraventricular thalamic nucleus in 936
the regulation of stress, motivation, and mood. *Front 937
Behav Neurosci* 8: 73, 2014. 938
Igelstrom KM, Herbison AE, Hyland BI. Enhanced c- 939
Fos expression in superior colliculus, paraventricular 940
thalamus and septum during learning of cue-reward 941
association. *Neuroscience* 168: 706–714, 2010. 942
Ishikawa A, Ambroggi F, Nicola SM, Fields HL. Contri- 943
butions of the amygdala and medial prefrontal cortex 944
to incentive cue responding. *Neuroscience* 155: 573– 945
584, 2008. 946
James MH, Dayas CV. What about me? The PVT: a 947
role for the paraventricular thalamus (PVT) in drug- 948
seeking behavior. *Front Behav Neurosci* 7: 18, 2013. 949
Kirouac GJ. Placing the paraventricular nucleus of the 950
thalamus within the brain circuits that control behav- 951
ior. *Neurosci Biobehav Rev* 56: 315–329, 2015. 952

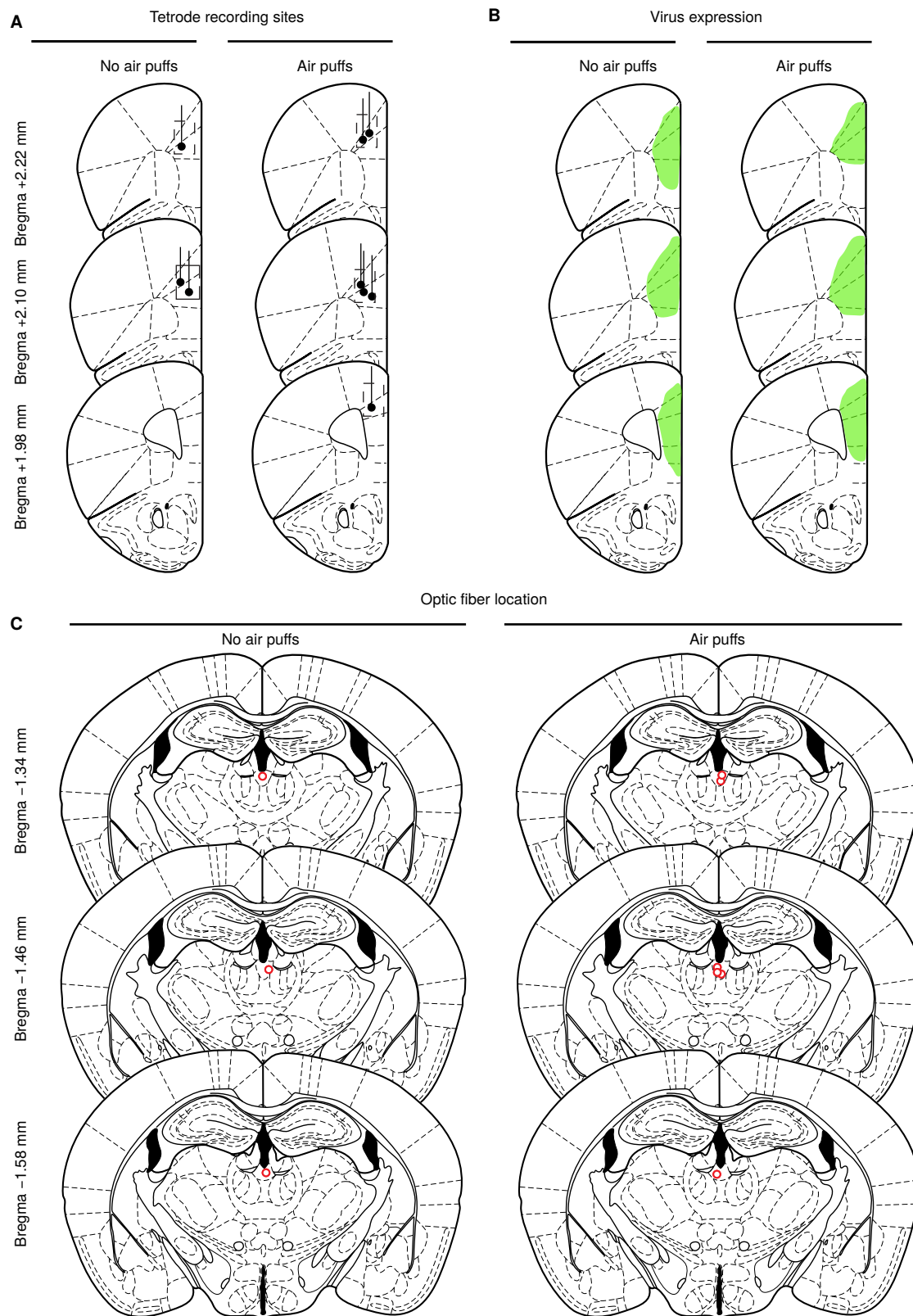
- 953 Kukolja J, Schläpfer TE, Keysers C, Klingmüller D, MacLeod A, Byrne A. Anxiety, depression, and the an- 996
954 Maier W, Fink GR, Hurlemann R. Modeling a ticipation of future positive and negative experiences. 997
955 negative response bias in the human amygdala by 998
956 noradrenergic-glucocorticoid interactions. *J Neurosci* 998
957 28: 12868–12876, 2008.
958 Lawson C, MacLeod C, Hammond G. Interpretation Martin-Fardon R, Boutrel B. Orexin/hypocretin 999
959 revealed in the blink of an eye: depressive bias in the (Orx/Hcrt) transmission and drug-seeking behavior: 1000
960 resolution of ambiguity. *J Abnorm Psychol* 111: 321– 1001
961 328, 2002. part of the drug seeking circuitry? *Front Behav Neu- 1002
962 Lee JH, Durand R, Gradinariu V, Zhang F, Goshen I, rosci* 6: 75, 2012. 1003
963 Kim DS, Fenno LE, Ramakrishnan C, Deisseroth K. Matzeu A, Weiss F, Martin-Fardon R. Transient inacti- 1004
964 Global and local fMRI signals driven by neurons de- vation of the posterior paraventricular nucleus of the 1005
965 fined optogenetically by type and wiring. *Nature* 465: thalamus blocks cocaine-seeking behavior. *Neurosci 1006
966 788–792, 2010. Lett* 608: 34–39, 2015. 1007
967 Lerner JS, Keltner D. Beyond valence: Toward a Moorman DE, Aston-Jones G. Prefrontal neurons en- 1008
968 model of emotion-specific influences on judgement and code context-based response execution and inhibition 1009
969 choice. *Cogn Emot* 14: 473–493, 2000. 1010
970 Levy I, Snell J, Nelson AJ, Rustichini A, Glimcher PW. *Proc Natl Acad Sci U S A* 112: 9472–9477, 2015. 1011
971 Neural representation of subjective value under risk and ambiguity. *J Neurophysiol* 103: 1036–1047, 2010.
972
973 Li S, Kirouac GJ. Sources of inputs to the anterior and Morgan MA, LeDoux JE. Differential contribution of 1012
974 posterior aspects of the paraventricular nucleus of the dorsal and ventral medial prefrontal cortex to the ac- 1013
975 thalamus. *Brain Struct Funct* 217: 257–273, 2012. quisition and extinction of conditioned fear in rats. 1014
976 Li Y, Lindemann C, Goddard MJ, Hyland BI. Complex *Behav Neurosci* 109: 681–688, 1995. 1015
977 Multiplexing of Reward-Cue- and Licking-Movement- Orsini CA, Heshmati SC, Garman TS, Wall SC, Bizon 1019
978 Related Activity in Single Midline Thalamus Neurons. JL, Setlow B. Contributions of medial prefrontal cor- 1020
979 *J Neurosci* 36: 3567–3578, 2016. tex to decision making involving risk of punishment. 1021
980 Liston C, Miller MM, Goldwater DS, Radley JJ, Rocher 1022
981 AB, Hof PR, Morrison JH, McEwen BS. Stress- *Neuropharmacology* 139: 205–216, 2018. 1022
982 induced alterations in prefrontal cortical dendritic 1023
983 morphology predict selective impairments in percep- Otis JM, Namboodiri VMK, Matan AM, Voets ES, Mo- 1024
984 tual attentional set-shifting. *J Neurosci* 26: 7870– horn EP, Kosyk O, McHenry JA, Robinson JE, Re- 1025
985 7874, 2006. sendez SL, Rossi MA, Stuber GD. Prefrontal cortex 1026
986 Liu RJ, Aghajanian GK. Stress blunts serotonin- and output circuits guide reward seeking through diver- 1027
987 hypocretein-evoked EPSCs in prefrontal cortex: role gent cue encoding. *Nature* 543: 103–107, 2017. 1027
988 of corticosterone-mediated apical dendritic atrophy. 1028
989 *Proc Natl Acad Sci U S A* 105: 359–364, 2008.
990 Luce RD. *Response Times: Their Role in Inferring Paintal A. Intramuscular propagation of sensory im- 1028
991 Elementary Mental Organization*. Oxford University pulses. *J Physiol* 148: 240–251, 1959. 1029
992 Press, 1986.
993 Luk CH, Wallis JD. Dynamic encoding of responses and Papciak J, Popik P, Fuchs E, Rygula R. Chronic psy- 1030
994 outcomes by neurons in medial prefrontal cortex. *J chosocial stress makes rats more ‘pessimistic’ in the 1031
995 Neurosci* 29: 7526–7539, 2009. ambiguous-cue interpretation paradigm. *Behav Brain 1032
996 Res* 256: 305–310, 2013. 1033
997 Parker RMA, Paul ES, Burman OHP, Browne WJ, 1034
998 Mendl M. Housing conditions affect rat responses to 1035
999 two types of ambiguity in a reward-reward discrimina- 1036
1000 tion cognitive bias task. *Behav Brain Res* 274: 73–83, 1037
1001 2014. 1038

- 1039 Penzo MA, Robert V, Tucciarone J, De Bundel D, Wang 1083
1040 M, Van Aelst L, Darvas M, Parada LF, Palmiter RD, How-
1041 He M, Huang ZJ, Li B. The paraventricular thalamus land JG. Alterations in reward, fear and safety cue
1042 controls a central amygdala fear circuit. *Nature* 519: discrimination after inactivation of the rat prelimbic 1084
1043 455–459, 2015. and infralimbic cortices. *Neuropsychopharmacology* 1085
1086 39: 2405–2413, 2014. 1087
- 1044 Peters J, Kalivas PW, Quirk GJ. Extinction circuits for 1088
1045 fear and addiction overlap in prefrontal cortex. *Learn-
1046 Mem* 16: 279–288, 2009. 1089
- 1047 Phillips ML, Drevets WC, Rauch SL, Lane R. Neuro- 1090
1048 biology of emotion perception I: The neural basis of
1049 normal emotion perception. *Biol Psychiat* 54: 504– 1091
1050 514, 2003. 1092
- 1051 Pizzagalli DA, Iosifescu D, Hallett LA, Ratner KG, Fava 1093
1052 M. Reduced hedonic capacity in major depressive dis-
1053 order: evidence from a probabilistic reward task. *J
1054 Psychiat Res* 43: 76–87, 2008. 1094
- 1055 Radley JJ, Rocher AB, Janssen WGM, Hof PR, McEwen 1095
1056 BS, Morrison JH. Reversibility of apical dendritic re-
1057 traction in the rat medial prefrontal cortex following
1058 repeated stress. *Exp Neurol* 196: 199–203, 2005. 1096
- 1059 Radley JJ, Rocher AB, Miller M, Janssen WGM, Lis- 1097
1060 ton C, Hof PR, McEwen BS, Morrison JH. Repeated
1061 stress induces dendritic spine loss in the rat medial
1062 prefrontal cortex. *Cereb Cortex* 16: 313–320, 2006. 1098
- 1063 Radley JJ, Rocher AB, Rodriguez A, Ehlenberger DB, 1099
1064 Dammann M, McEwen BS, Morrison JH, Wearne SL,
1065 Hof PR. Repeated stress alters dendritic spine mor-
1066 phology in the rat medial prefrontal cortex. *J Comp
1067 Neurol* 507: 1141–1150, 2008. 1100
- 1068 Radley JJ, Sisti HM, Hao J, Rocher AB, McCall T, Hof 1101
1069 PR, McEwen BS, Morrison JH. Chronic behavioral
1070 stress induces apical dendritic reorganization in pyra-
1071 midal neurons of the medial prefrontal cortex. *Neuro-
1072 science* 125: 1–6, 2004. 1102
- 1073 Rygula R, Papciak J, Popik P. Trait pessimism predicts 1103
1074 vulnerability to stress-induced anhedonia in rats. *Neu-
1075ropsychopharmacology* 38: 2188–2196, 2013. 1104
- 1076 Rygula R, Papciak J, Popik P. The effects of acute 1105
1077 pharmacological stimulation of the 5-HT, NA and DA
1078 systems on the cognitive judgement bias of rats in
1079 the ambiguous-cue interpretation paradigm. *Eur Neu-
1080 psychopharmacol* 24: 1103–1111, 2014. 1106
- 1081 Rygula R, Pluta H, Popik P. Laughing rats are opti- 1107
1082 mistic. *PLoS One* 7: e51959, 2012. 1108
- 1083 Sangha S, Robinson PD, Greba Q, Davies DA, How-
1084 land JG. Alterations in reward, fear and safety cue
1085 discrimination after inactivation of the rat prelimbic
1086 and infralimbic cortices. *Neuropsychopharmacology* 1087
1088 39: 2405–2413, 2014. 1089
- 1089 Schiltz CA, Bremer QZ, Landry CF, Kelley AE. Food-
1090 associated cues alter forebrain functional connec-
1091 tivity as assessed with immediate early gene and
1092 proenkephalin expression. *BMC Biol* 5: 16, 2007. 1093
- 1092 Schiltz CA, Kelley AE, Landry CF. Contextual cues 1094
1093 associated with nicotine administration increase arc
1094 mRNA expression in corticolimbic areas of the rat
1095 brain. *Eur J Neurosci* 21: 1703–1711, 2005. 1096
- 1096 Schmitzer-Torbert N, Jackson J, Henze D, Harris K, Re- 1097
1097 dish A. Quantitative measures of cluster quality for
1098 use in extracellular recordings. *Neuroscience* 131: 1– 1099
1099 11, 2005. 1100
- 1099 Schwarz N, Clore GL. Mood, misattribution, and judg-
1100 ments of well-being: informative and directive func-
1101 tions of affective states. *J Personal Soc Psychol* 45:
1102 513, 1983. 1103
- 1104 Sharp FR, Sagar SM, Hicks K, Lowenstein D, Hisanaga
1105 K. c-fos mRNA, Fos, and Fos-related antigen induc-
1106 tion by hypertonic saline and stress. *J Neurosci* 11:
1107 2321–2331, 1991. 1108
- 1108 Sierra-Mercado D, Padilla-Coreano N, Quirk GJ. Disso-
1109 ciable roles of prelimbic and infralimbic cortices, ven-
1110 tral hippocampus, and basolateral amygdala in the
1111 expression and extinction of conditioned fear. *Neu-
1112 psychopharmacology* 36: 529–538, 2011. 1113
- 1113 Sotres-Bayon F, Quirk GJ. Prefrontal control of fear: 1114
1114 more than just extinction. *Curr Opin Neurobiol* 20:
1115 231–235, 2010. 1116
- 1116 Sparta DR, Hovelsø N, Mason AO, Kantak PA, Ung RL,
1117 Decot HK, Stuber GD. Activation of prefrontal corti-
1118 cal parvalbumin interneurons facilitates extinction of
1119 reward-seeking behavior. *J Neurosci* 34: 3699–3705,
1120 2014. 1121
- 1121 Spencer SJ, Fox JC, Day TA. Thalamic paraventricular
1122 nucleus lesions facilitate central amygdala neuronal re-
1123 sponds to acute psychological stress. *Brain Res* 997:
1124 234–237, 2004. 1125

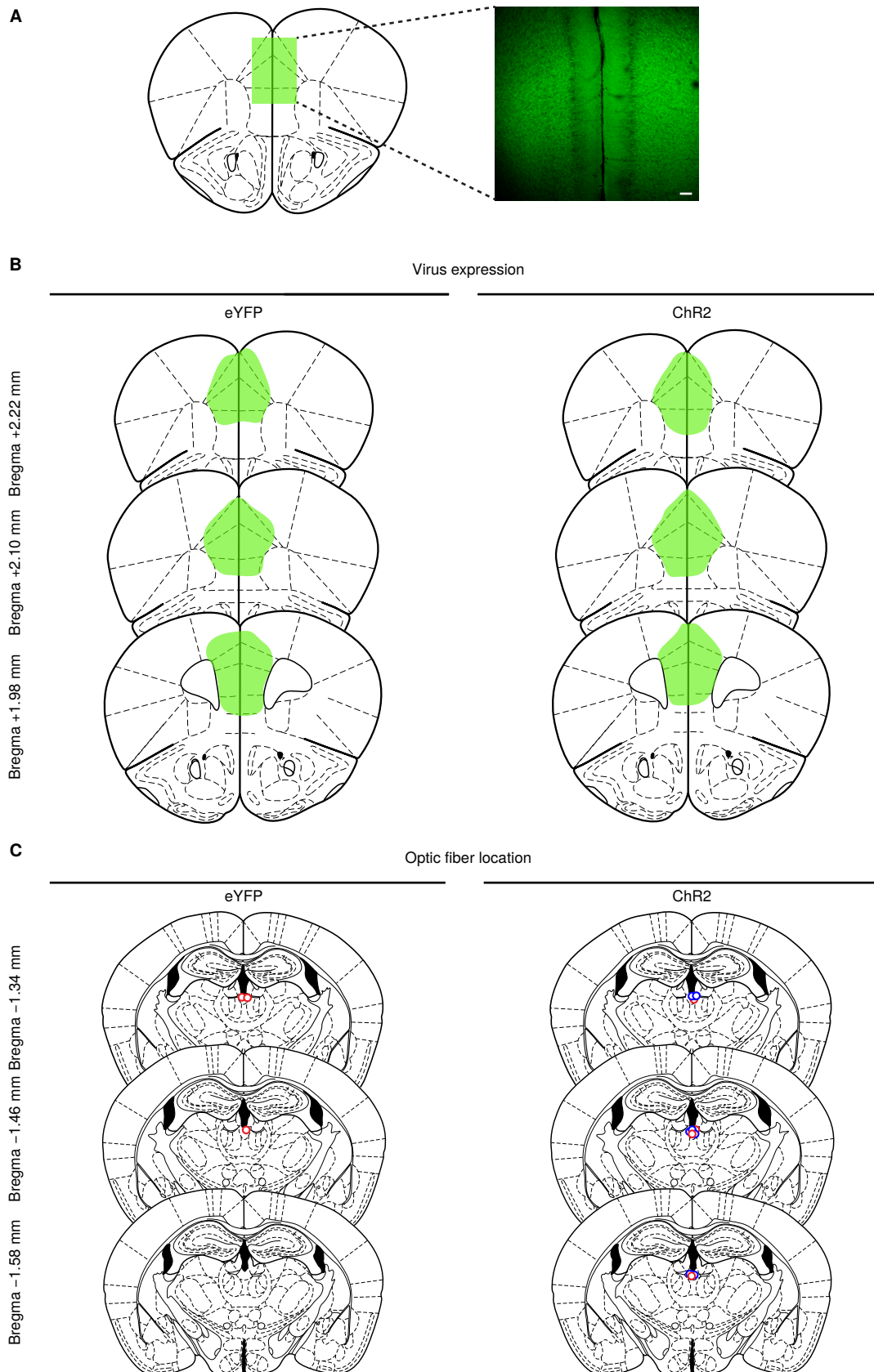
- 1125 Stoelzel CR, Bereshpolova Y, Alonso JM, Swadlow HA.
1126 Axonal Conduction Delays, Brain State, and Cortico-
1127 geniculate Communication. *J Neurosci* 37: 6342–
1128 6358, 2017.
- 1129 Sugrue LP, Corrado GS, Newsome WT. Choosing the
1130 greater of two goods: neural currencies for valuation
1131 and decision making. *Nat Rev Neurosci* 6: 363–375,
1132 2005.
- 1133 Swadlow HA. Neocortical efferent neurons with very
1134 slowly conducting axons: strategies for reliable an-
1135 tidromic identification. *J Neurosci Meth* 79: 131–141,
1136 1998.
- 1137 Swadlow HA, Weyand TG. Efferent systems of the rab-
1138 bit visual cortex: laminar distribution of the cells of
1139 origin, axonal conduction velocities, and identification
1140 of axonal branches. *J Comp Neurol* 203: 799–822,
1141 1981.
- 1142 Vertes RP. Differential projections of the infralimbic and
1143 prelimbic cortex in the rat. *Synapse* 51: 32–58, 2004.
- 1144 Wei Q, Hebda-Bauer EK, Pletsch A, Luo J, Hoversten
1145 MT, Osetek AJ, Evans SJ, Watson SJ, Seasholtz AF,
1146 Akil H. Overexpressing the glucocorticoid receptor in
1147 forebrain causes an aging-like neuroendocrine pheno-
1148 type and mild cognitive dysfunction. *J Neurosci* 27:
1149 8836–8844, 2007.
- 1150 Wellman CL. Dendritic reorganization in pyramidal neu-
1151 rons in medial prefrontal cortex after chronic corticos-
1152 terone administration. *J Neurobiol* 49: 245–253, 2001.
- 1153 Wright WF, Bower GH. Mood effects on subjective
1154 probability assessment. *Organiz Behav Hum Decis
1155 Proc* 52: 276–291, 1992.
- 1156 Yasoshima Y, Scott TR, Yamamoto T. Differential acti-
1157 vation of anterior and midline thalamic nuclei follow-
1158 ing retrieval of aversively motivated learning tasks.
1159 *Neuroscience* 146: 922–930, 2007.
- 1160 Yuen EY, Wei J, Liu W, Zhong P, Li X, Yan Z. Repeated
1161 stress causes cognitive impairment by suppressing glu-
1162 tamate receptor expression and function in prefrontal
1163 cortex. *Neuron* 73: 962–977, 2012.
- 1164 Zhu Y, Wienecke CFR, Nachtrab G, Chen X. A thala-
1165 mic input to the nucleus accumbens mediates opiate
1166 dependence. *Nature* 530: 219–222, 2016.
- 1167
- Author contributions** F.L., Z.S., A.J.C., and
1168 B.A.B. collected data. F.L. and J.Y.C. designed exper-
1169 iments, analyzed data, and wrote the paper.
1170
- Author information** Correspondence should be ad-
1171 dressed to J.Y.C. (jeremiah.cohen@jhmi.edu).
1172
- 1173



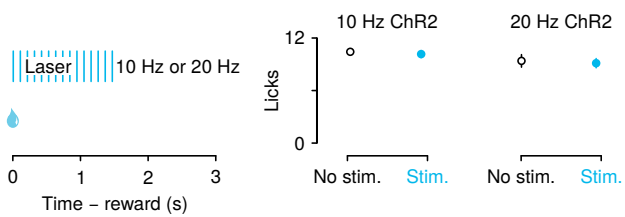
Supplementary Figure 1 | Drawings illustrate recording sites in mPFC in no air puff (left) and air puff exposed (right) mice. Boxes indicate approximate location of recording sites in each mouse, taking into account any vertical distance traveled during training and the approximate lateral spread of the tetrode bundle.



Supplementary Figure 2 | (A) Drawings illustrate recording sites in mPFC in no air puff (left, N=3) and air puff exposed (right, N=6) mice. Boxes indicate approximate location of recording sites in each mouse, taking into account any vertical distance traveled during training and the approximate lateral spread of the tetrode bundle. (B) Traces showing virus expression in no air puff (left) and air puff (right) groups. (C) Locations of fiber tips in no air puff (left) and air puff (right) groups in PVT.



Supplementary Figure 3 | (A) Schematic drawing of viral stereotaxic injection into mPFC. Inset: eYFP (green) expression in a mPFC coronal section from a BL6 mouse that received AAV1-CaMKII α -ChR2-eYFP into mPFC (scale bar, 50 μ m). (B) Traces showing the expression of eYFP (left) and ChR2-eYFP (right) groups. (C) Locations of fiber tips in eYFP (left) and ChR2-eYFP (right, red=10 Hz and blue=20 Hz) groups in PVT.



Supplementary Figure 4 | mPFC→PVT stimulation did not suppress licking for unexpected rewards. Left: optical stimulation was delivered during the presentation of reward delivery and lasted for 1500 ms, Right: licking behavior in 10 Hz ChR2-eYFP (left) and 20 Hz ChR2-eYFP (right) groups across trials with no stimulation (black) and trials with stimulation (light blue). Line and error bars represent the mean \pm SEM.